

Electronic Supporting Information (ESI)

## **Self-Assembled DNA Nanocentipede as Multivalent Vehicle for Enhanced Delivery of CpG Oligonucleotides**

Wenshan Li, Lei Luo, Jin Huang, Qing Wang, Jianbo Liu, Xiao Xiao, Hongmei Fang, Xiaohai Yang\* and Kemin Wang\*

*State Key Laboratory of Chemo/Biosensing and Chemometrics, College of Chemistry and Chemical Engineering, Key Laboratory for Bio-Nanotechnology and Molecular Engineering of Hunan Province, Hunan University, Changsha 410082, China*

### **Contents of ESI:**

#### **Experimental Section**

- S1** Chemicals and Materials
- S2** Cell Lines and Buffers
- S3** Preparation of CpG-Nces
- S4** Agarose Gel Electrophoresis
- S5** Cytotoxicity Assay
- S6** Confocal Fluorescence Microscopy Imaging
- S7** Three-Dimensional Reconstruction
- S8** Uptake of CpG-Nces in RAW264.7 Cells
- S9** Stability of CpG-Nces
- S10** Cytokine Secretion from RAW264.7 cells
- S11** Immunotherapeutic Effect
- S12** Statistical Analysis

#### **Table and Figures**

**Table S1** Sequences of DNA probes.

**Fig. S1** Agarose gel electrophoresis showing the formation of CpG-Nces.

**Fig. S2** Effects of CpG-Nces on proliferation of RAW64.7 cells.

**Fig. S3** Characterization of the time-dependent internalization of CpG-Nces in RAW264.7 cells.

**Fig. S4** Internalized CpG(200)-Nces in RAW264.7 Cells at different Z positions revealed by confocal microscopy.

**Fig. S5** Characterization of the temperature-dependent internalization of CpG(200)-Nces in RAW264.7 cells.

**Fig. S6** Colocalization studies of the internalization of CpG(200)-Nces and free CpG ODNs in RAW264.7 cells.

**Fig. S7** Effects of the valence number of CpG-Nces on cellular uptake revealed by flow cytometry.

**Fig. S8** Colocalization studies of the stability of CpG-Nces within cells.

**Fig. S9** Serum stability of CpG(200)-Nces compared with free CpG ODNs.

**Fig. S10** Effect of different CpG(200)-Nces concentrations on immunostimulation.

**Fig. S11** Effect of incubate time on immunostimulation.

**Fig. S12** Characterization of the long-lasting immunostimulatory activities of CpG(200)-Nces.

**Fig. S13** The therapeutic effect of CpG-Nces on cancer cells revealed by flow cytometry.

**Fig. S14** The therapeutic effect of CpG(200)-Nces on cancer cells revealed by confocal microscopy.

**Fig. S15** Effect of co-culture time on immunotherapy at 37 °C.

**Fig. S16** Characterization of time-dependent immunotherapeutic effect of CpG(200)-Nces.

## **Experimental Section**

### **S1 Chemicals and Materials**

All DNA oligonucleotides were synthesized and HPLC purified by Sangon Biotech. Co. Ltd. (Shanghai, China), and dissolved in phosphate buffered saline (PBS) solution (10 mM phosphate buffer, 137 mM NaCl, 2.7 mM KCl, pH 7.4). The sequences of the oligonucleotides are listed in Table 1. Streptavidin and 3-(4, 5-Dimethylthiazol-2-yl)-2, 5-diphenyltetrazolium bromide (MTT) were purchased from Sigma-Aldrich (USA). Hoechst 33342 (Hoechst) and SYBR<sup>®</sup> Gold were purchased from Invitrogen (USA). Bovine serum albumin (BSA) and yeast tRNA were purchased from Dingguo Changsheng Biotechnology Co., Ltd. (Beijing, China). All other reagents were the highest grade available. All solutions were prepared and diluted using ultrapure water ( $\geq 18.2$  M $\Omega$  cm) from the Millipore Milli-Q system (Barnstead/Thermolyne NANO-pure, Dubuque, IA). Washing buffer contained glucose (4.5 g/L) and MgCl<sub>2</sub> (5 mM) in PBS solution. Binding buffer was prepared by adding yeast tRNA (0.1 mg/mL) and BSA (1 mg/mL) to the washing buffer to reduce background binding.

### **S2 Cell Lines and Buffers**

Murine macrophage (RAW264.7) cells and T lymphoblast leukemia (CCRF-CEM) cells were purchased from the Shanghai Institute of Cell Biology of the Chinese Academy of Science. RAW264.7 cells were cultured in high glucose Dulbecco's modified Eagle's medium (DMEM, Sigma-Aldrich) supplemented with 10% fetal bovine serum (FBS; heat-inactivated) and 1.5 g/L NaHCO<sub>3</sub>. CCRF-CEM cells were cultured in RPMI medium 1640 supplemented with 10% fetal bovine serum (FBS; heat-inactivated), 100 units/mL penicillin and 100  $\mu$ g/mL streptomycin. Both cultures were incubated at 37 °C under a 5% CO<sub>2</sub> atmosphere.

### **S3 Preparation of CpG-Nces**

H1 and H2 were dissolved in PBS to a common final concentration of 100  $\mu$ M, heated to 96 °C for 3 min, immediately cooled on ice for 3 min, and then left at room temperature for 2 h before use. Trigger (250 nM) were incubated with H1 (25  $\mu$ M) and H2 (25  $\mu$ M) at 25 °C for 24 h, then dilute with PBS, followed by incubating with streptavidin and biotinylated CpG ODNs at 25 °C for 2 h.

### **S4 Agarose gel electrophoresis**

A 2% agarose gel was prepared using a 1  $\times$  TAE buffer (40 mM Tris AcOH, 2.0 mM Na<sub>2</sub>EDTA, pH 8.5). The SYBR<sup>®</sup> Gold was used as oligonucleotide dye. The gel was run at 100 V for 60 min in 1  $\times$  TAE buffer at room temperature, and then photographed in Gel Imaging (Tanon 2500 R, Tianneng Ltd., Shanghai, China).

### **S5 Cytotoxicity Assay**

*In vitro* cytotoxicity was determined using MTT assay. Briefly, cells were seeded at  $1 \times 10^4$  cells per well into 96-well plates for 24 h. Then, cells were treated with

CpG-Nces or Lib-Nces in medium (without FBS, unless denoted otherwise; 37 °C; 5% CO<sub>2</sub>) for 24 h. After removing cell medium, 20 µL of MTT solution (5 mg/mL) diluted in fresh medium (100 µL) was added to each well and incubated for 4 h. The precipitated formazan violet crystals were dissolved in 150 µL of DMSO. The absorbance value at 570 nm was recorded using a multi-function plate reader Benchmarks Plus (BIO-RAD, USA). Each concentration was tested at least three times.

### **S6 Confocal Fluorescence Microscopy Imaging**

All cellular fluorescent images were collected on a FV 500-IX70 confocal microscope (Olympus America Inc., Melville, NY) with a 100× oil immersion objective (Olympus, Melville, NY). Excitation wavelength and emission filters: Hoechst or LysoTracker<sup>®</sup> Blue channel: EX 405 nm, emission bandpass (430-460 nm) filter. FITC: EX 488 nm, emission bandpass (505–525 nm) filter. TAMRA EX 543 nm, emission bandpass (565 nm long-pass) filter. RAW264.7 cells were plated in a 35 mm confocal dish and grown to around 80% confluency before the experiment. Cells were incubated with samples at 37 °C for various time points. After the medium was removed, the cells were washed twice with washing buffer, followed by Hoechst or LysoTracker<sup>®</sup> Blue staining, and visualized under a confocal laser scanning microscope.

### **S7 Three-Dimensional Reconstruction**

All cellular fluorescent images were collected on a FV 500-IX70 confocal microscope (Olympus America Inc., Melville, NY) with a 100× oil immersion objective (Olympus, Melville, NY). Excitation wavelength and emission filters: TAMRA EX 543 nm, emission bandpass (565 nm long-pass) filter. RAW264.7 cells were plated in a 35 mm confocal dish and grown to around 80% confluency before the experiment. Cells were incubated with CpG(200)-Nces (100 nM TAMRA-labeled CpG equivalents) at 37 °C for 4 h. After the medium was removed, the cells were washed twice with washing buffer. 3D reconstitution of Z-axis scanning was performed using the ImageJ software (NIH, Bethesda, MD, USA).

### **S8 Uptake of CpG-Nces in RAW264.7 Cells**

FITC-labeled H1 and H2 were used for the preparation of fluorescently labeled DNA nanostructures. RAW264.7 cells were seeded on 24-well culture plates at a density of  $1 \times 10^5$  cells/mL (1 mL) and cultured for 24 h and then washed twice with PBS. They were incubated with fluorescently labeled DNA structures for 4 h at 37 °C, harvested, and washed three times with PBS. Then, the fluorescence intensity of the cells was determined by flow cytometry (Beckman Coulter, USA).

### **S9 Stability of CpG-Nces**

For stability investigation, CpG(200)-Nces and CpG ODNs were incubated with 50% human serum diluted in PBS at 37 °C for difference times. The reaction was then stopped with a final concentration of 20 mM EDTA. Finally, the samples were then loaded on a 2% agarose gel and subjected to electrophoresis as described above.

### **S10 Cytokine Secretion from RAW264.7 cells**

RAW264.7 cells were seeded on 24-well culture plates at a density of  $1 \times 10^5$  cells/mL per well (1 mL) in fresh medium and incubated for 24 h. Cells were then washed twice with 1 mL PBS before treatment with the indicated conditions and incubated at 37 °C for the indicated time. The media were collected afterwards and centrifuged at 12,000 rpm for 20 min at 4 °C (Microfuge<sup>®</sup> 18, Beckman Coulter, USA). The levels of TNF- $\alpha$  and IL-6 were measured using ELISA kits (VAL609, VAL604, R&D Systems) following protocols recommended by the manufacturer.

### **S11 Immunotherapeutic Effect**

RAW264.7 cells were seeded on 24-well culture plates at a density of  $1 \times 10^5$  cells/mL per well (1 mL) in fresh medium and incubated for 24 h. After washing twice with PBS, CEM cells at a density of  $2 \times 10^5$  cells per well mixed with the indicated therapeutics in fresh DMEM medium were incubated with the RAW264.7 cells for the indicated time. The cells in supernatant medium were collected and washed twice with PBS. Cell apoptosis was evaluated using FITC Annexin V Apoptosis Kit I (No. 556547, BD Pharmingen) by following the procedure recommended by the manufacturer and using flow cytometer (Beckman Coulter, USA). FITC and PI were excited at 488 nm; FITC was detected at FL1 (533/30 nm) while PI was detected at FL3 (>670 nm).

### **S12 Statistical Analysis**

All data were presented as mean  $\pm$  standard deviation and were evaluated by Student's t-test. A *p* value of less than 0.05 was considered to be statistically significant.

## **Table and Figures**

**Table S1. Sequences of DNA probes.**

Probes	Sequences (5'-3')
H1	<i>Biotin</i> -CGT CGT <u>GCA GCA GCA GCA GCA GCA</u> ACG GCT <u>TGC TGC TGC TGC TGC</u>
FITC-labeled H1	<i>Biotin</i> -CGT CGT <u>GCA GCA GCA GCA GCA GCA</u> ACG GCT <u>TGC TGC TGC TGC TGC</u> -FITC
H2	<i>Biotin</i> - <u>TGC TGC TGC TGC TGC TGC</u> ACG ACG <u>GCA GCA GCA GCA GCA GCA</u> AGC CGT
FITC-labeled H2	<i>Biotin</i> - <u>TGC TGC TGC TGC TGC TGC</u> ACG ACG <u>GCA GCA GCA GCA GCA GCA</u> AGC CGT-FITC
Trigger	TGC TGC TGC TGC TGC TGC ACG ACG
CpG ODN	TCC ATG ACG TTC CTG ACG TT (T) <sub>10</sub> - <i>Biotin</i>
TAMRA-labeled CpG ODN	<i>TAMRA</i> - TCC ATG ACG TTC CTG ACG TT (T) <sub>10</sub> - <i>Biotin</i>
Lib	(N) <sub>20</sub> (T) <sub>10</sub> - <i>Biotin</i>
TAMRA-labeled Lib	<i>TAMRA</i> -(N) <sub>20</sub> (T) <sub>10</sub> - <i>Biotin</i>

<sup>a</sup> TAMRA, if applicable, was labeled at the 5'-ends of CpG and Lib, FITC, if applicable, was labeled at the 3'-ends of H1 and H2. The underlined of DNA probes represent the stem complementary sequence of the hairpins.

## Figures

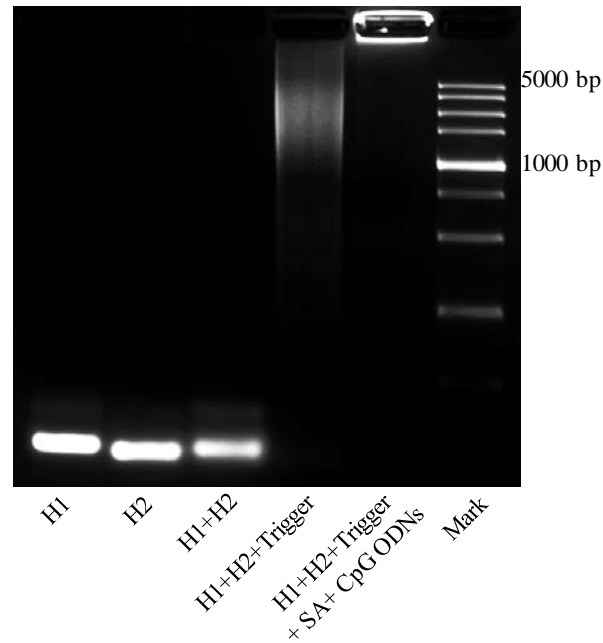


**Fig. S1** Agarose gel electrophoresis showing the formation of CpG-Nces.

From left to right lanes: (1) 50  $\mu$ M H1; (2) 50  $\mu$ M H2; (3) 25  $\mu$ M H1 + 25  $\mu$ M H2; (4) 25  $\mu$ M H1 + 25  $\mu$ M H2 + 250 nM Trigger; (5) 25  $\mu$ M H1 + 25  $\mu$ M H2 + 250 nM Trigger + 2  $\mu$ M streptavidin (SA) + 2  $\mu$ M biotinylated CpG ODNs, (6) DNA Markers. The samples were diluted 25-fold with PBS, followed by 2% agarose gel electrophoresis and visualized with SYBR<sup>®</sup> Gold staining.

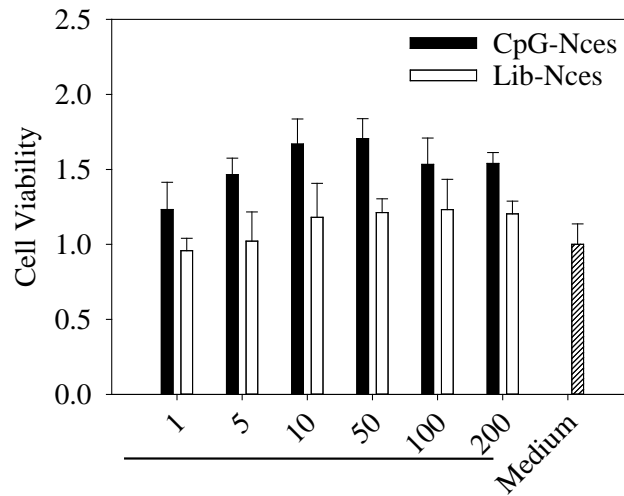


**Fig. S2** Effects of CpG-Nces on proliferation of RAW64.7 cells.

CpG-Nces (100 nM CpG ODN equivalents) and control Lib-Nces (100 nM Lib equivalents) were incubated with RAW264.7 cells at 37 °C for 24 h, respectively. The valence number of nanocentipede means the number of CpG ODN or Lib per nanocentipede. The results showed that the multivalent CpG-Nces (i.e. CpG(5)-Nces, CpG(10)-Nces, CpG(50)-Nces, CpG(100)-Nces, CpG(200)-Nces) could induce significant enhancement of cell proliferation. In contrast, monovalent CpG-Nces (i.e. CpG(1)-Nces) and Lib-Nces did not induce significant change of cell proliferation. The error bars indicated the standard deviations of three experiments. \* $p < 0.05$ ; \*\* $p < 0.001$  significantly different from medium group.



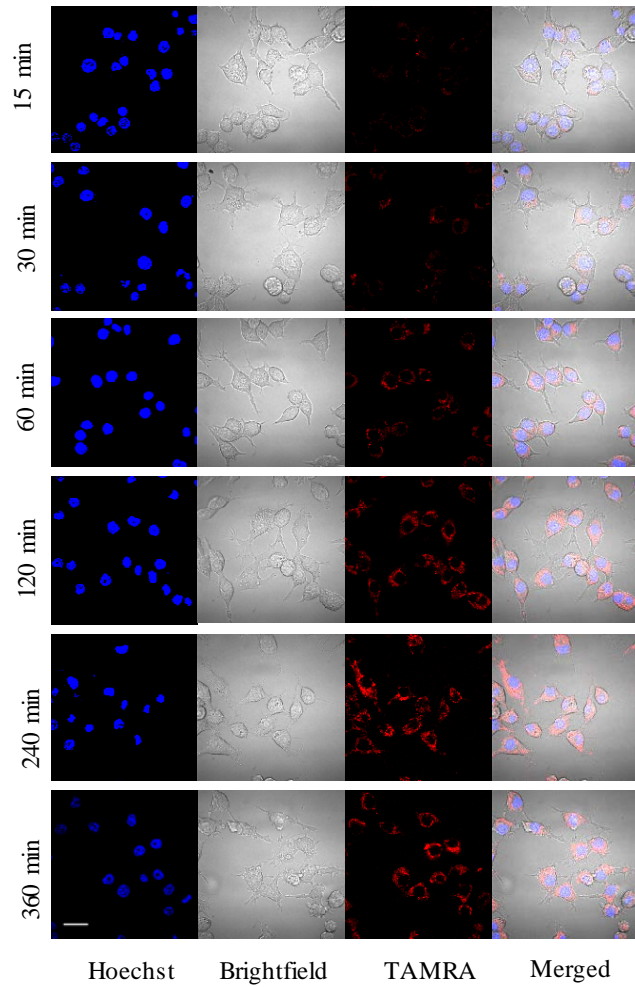


**Fig. S3** Characterization of the time-dependent internalization of CpG-Nces in RAW264.7 cells.

RAW264.7 cells were incubated with CpG(200)-Nces (100 nM TAMRA-labeled CpG ODN equivalents) at 37 °C for different times. Confocal microscopy images showed that the fluorescence intensity of cells was gradually enhanced with the increase of time. Scale bar: 20  $\mu$ m.

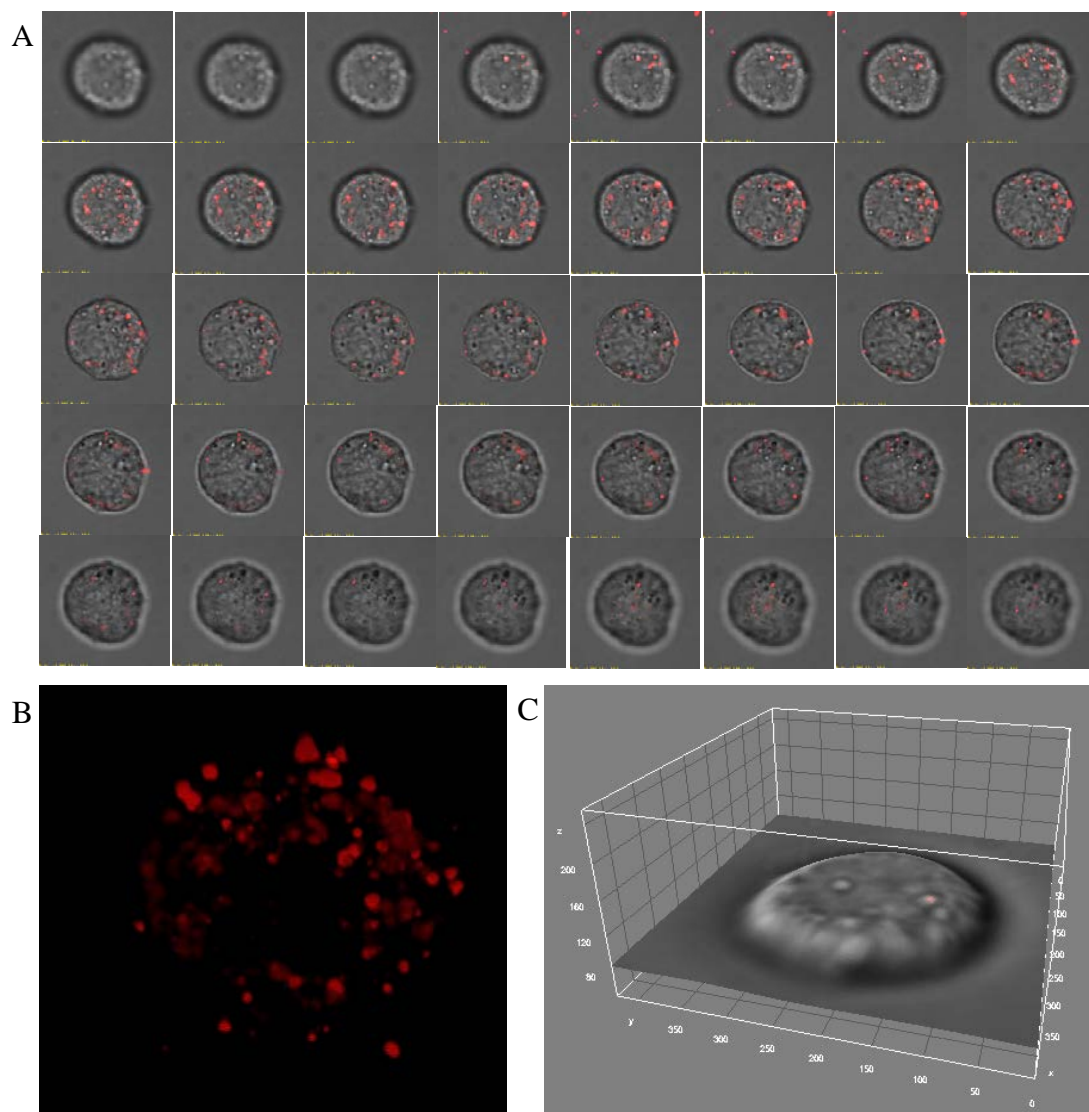


**Fig. S4** Internalized CpG(200)-Nces in RAW264.7 Cells at different Z positions revealed by confocal microscopy.

(A) As the Z-axis moves from bottom to top, the fluorescence of TAMRA was observed in RAW264.7 cell. (B) Three-dimensional reconstruction of the confocal Z-axis imaging of RAW263.7 cell without bright field. (C) Interactive 3D surface plot analysis of RAW263.7 cell with bright field. The results showed the distribution of TAMRA fluorescence within the cytoplasm rather than adsorbed on the membrane of RAW 264.7 cell.

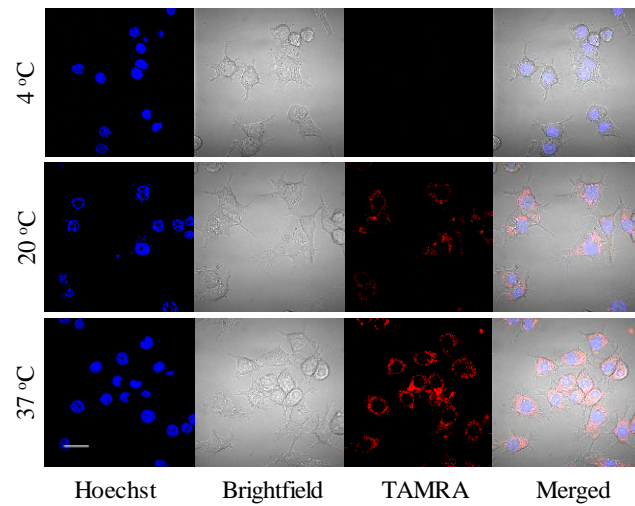


**Fig. S5** Characterization of the temperature-dependent internalization of CpG(200)-Nces in RAW264.7 cells.

RAW264.7 cells were incubated with CpG(200)-Nces (100 nM TAMRA-labeled CpG ODN equivalents) at different temperature for 4 h. Confocal microscopy images showed that the fluorescence intensity of cells was gradually enhanced with the increase of temperature. Scale bar: 20  $\mu\text{m}$ .

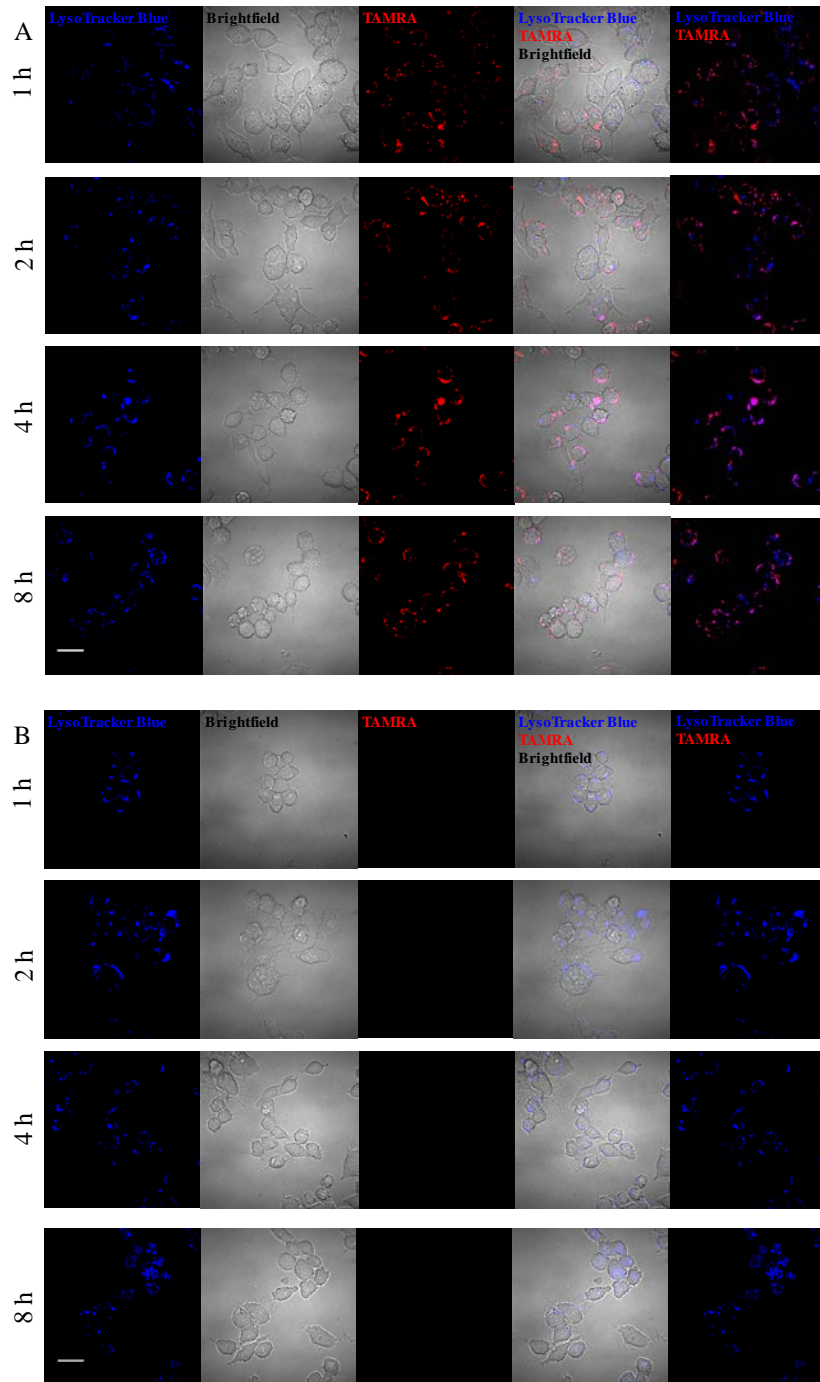


**Fig. S6** Colocalization studies of the internalization of CpG(200)-Nces (A) and free CpG ODNs (B) in RAW264.7 cells. Scale bar: 20  $\mu$ m.

RAW264.7 cells were incubated with CpG(200)-Nces (100 nM TAMRA-labeled CpG ODN equivalents) or free CpG ODNs (100 nM TAMRA-labeled CpG ODN) at 37 °C for 1, 2, 4, and 8 h, respectively. When RAW264.7 cells were treated with CpG(200)-Nces for more than 4 h, most of the red fluorescence from CpG(200)-Nces overlapped with the blue fluorescence from LysoTracker<sup>®</sup> Blue (stain acidic compartments in live cells), which indicated that CpG(200)-Nces were localized to late endosome/lysosomes. In contrast, free CpG ODNs were not efficiently uptaken by RAW264.7 cells.

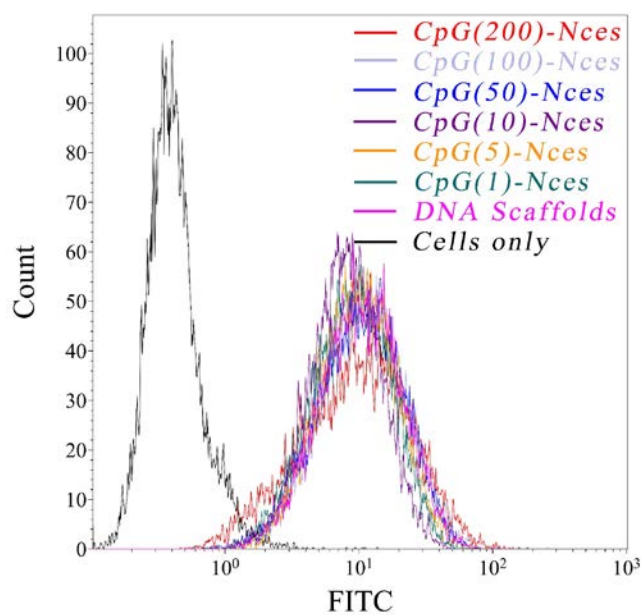


**Fig. S7** Effects of the valence number of CpG-Nces on cellular uptake revealed by flow cytometry.

At a given concentration of FITC-labeled H1/H2 (20 nM each) and Trigger (0.2 nM), RAW264.7 cells were incubated with different CpG-Nces or DNA scaffolds at 37 °C for 4 h, respectively. There was no measurable difference in the cellular uptake.

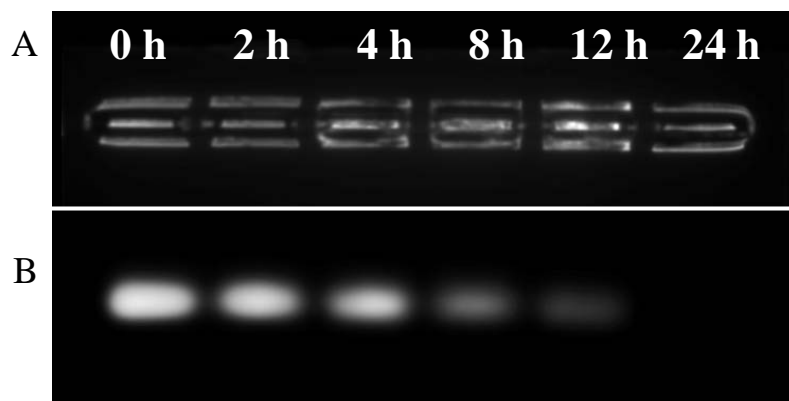


**Fig. S8** Serum stability of (A) CpG(200)-Nces compared with (B) free CpG ODNs.

The samples were incubated with 50% human serum at 37 °C for different times. The reaction mixtures were visualized with SYBR® Gold staining and analysed using 2% agarose gel electrophoresis.

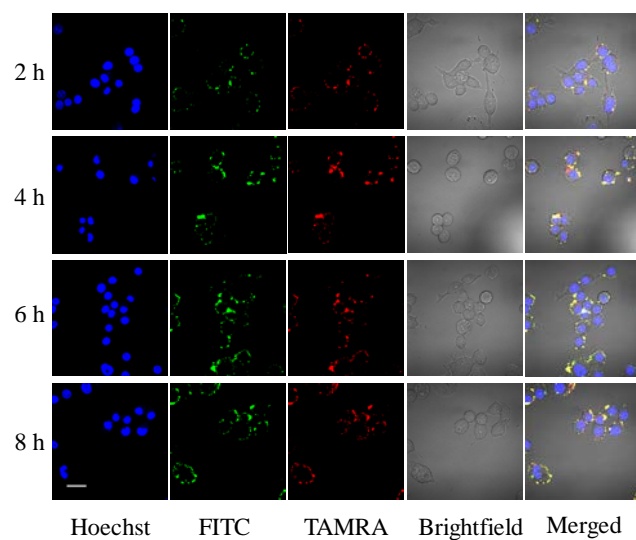


**Fig. S9** Colocalization studies of the stability of CpG-Nces within cells.

RAW264.7 cells were incubated with dual-labeled CpG(200)-Nces at 37 °C for different times. The FITC-labeled H1/H2 (50 nM, each) and TAMRA-labeled CpG ODNs (100 nM) to provide fluorescent tracing (FITC-green and TAMRA-red). Confocal microscopy images showed that the two fluorescent colors were present nearly in the same place even after 8 h. Scale bar: 20  $\mu$ m

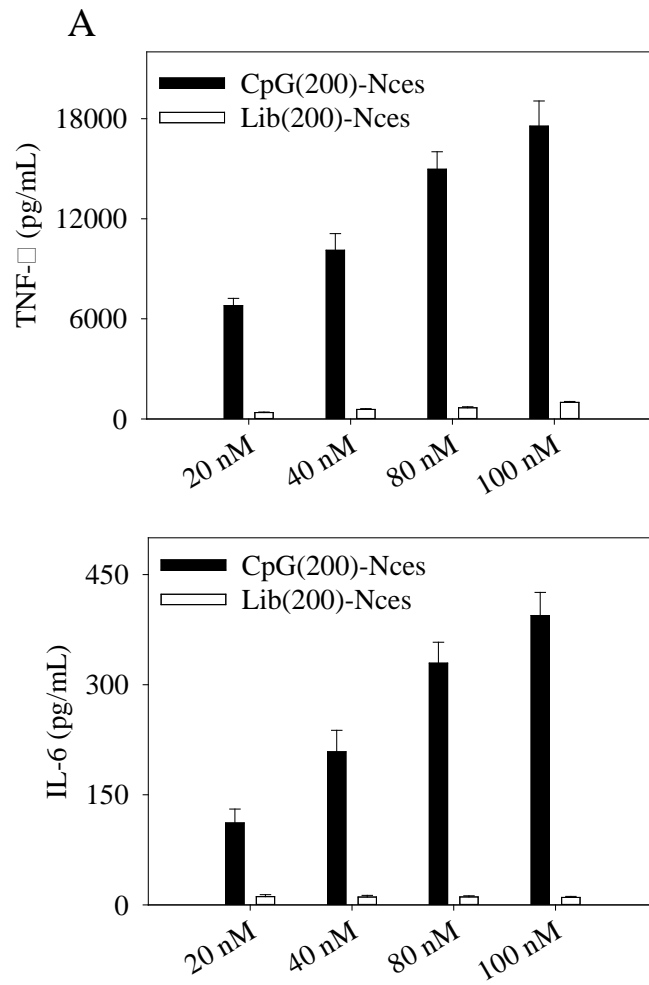


**Fig. S10** Effect of different CpG(200)-Nces concentrations on immunostimulation.

RAW 264.7 cells were incubated with different concentrations of CpG(200)-Nces (20, 40, 80, 100 nM CpG equivalents) and Lib(200)-Nces (20, 40, 80, 100 nM Lib equivalents) at 37 °C for 24 h, then the secretion levels of TNF- $\alpha$  (A) and IL-6 (B) were determined. The error bars indicated the standard deviations of three experiments.  $**p < 0.001$  significantly different from Lib(200)-Nces.



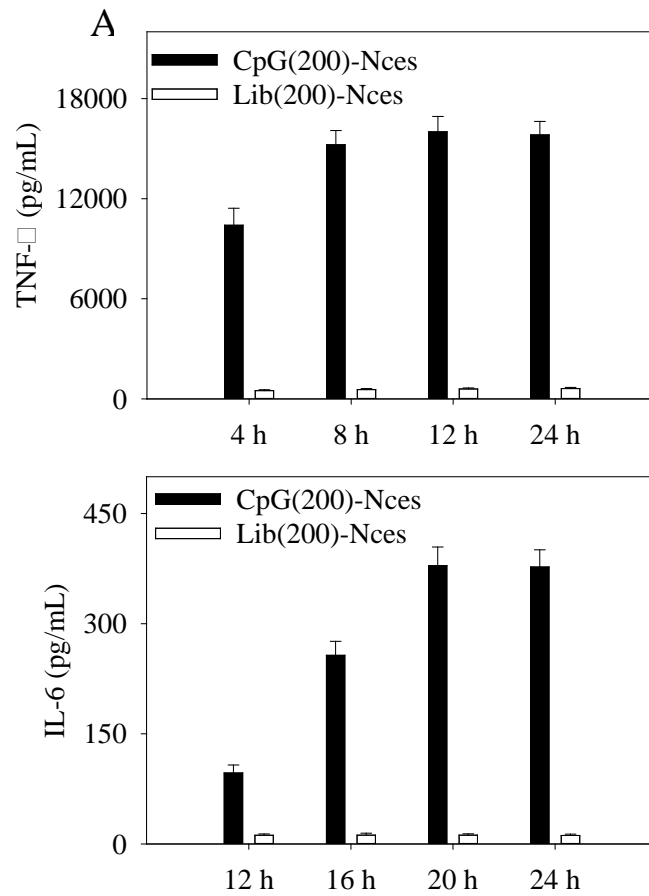


**Fig. S11** Effect of incubate time on immunostimulation.

CpG(200)-Nces (100 nM CpG equivalents) and Lib(200)-Nces (100 nM Lib equivalents) were incubated with RAW 264.7 cells at 37 °C for different time, then the secretion levels of TNF-α (A) and IL-6 (B) were determined. The error bars indicated the standard deviations of three experiments. \*\* $p < 0.001$  significantly different from Lib(200)-Nces.

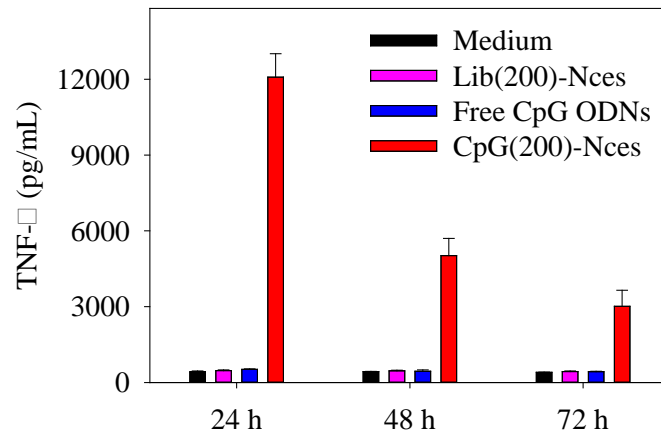


**Fig. S12 Characterization of the time-dependent immunostimulatory activities of CpG(200)-Nces.**

RAW264.7 cells were incubated with CpG(200)-Nces at 37 °C for 4 h. Cells were then washed twice with 1 mL PBS and fresh cell culture medium was added. After 24 h incubation, the media were collected. This process was repeated every 24 h over the course of 72 h. All the supernatants were collected and stored at -80 °C before assays. These results suggested that the secretion levels of TNF- $\alpha$  from RAW264.7 cells stimulated by CpG(200)-Nces were higher than that stimulated by free CpG ODNs at 72 h.

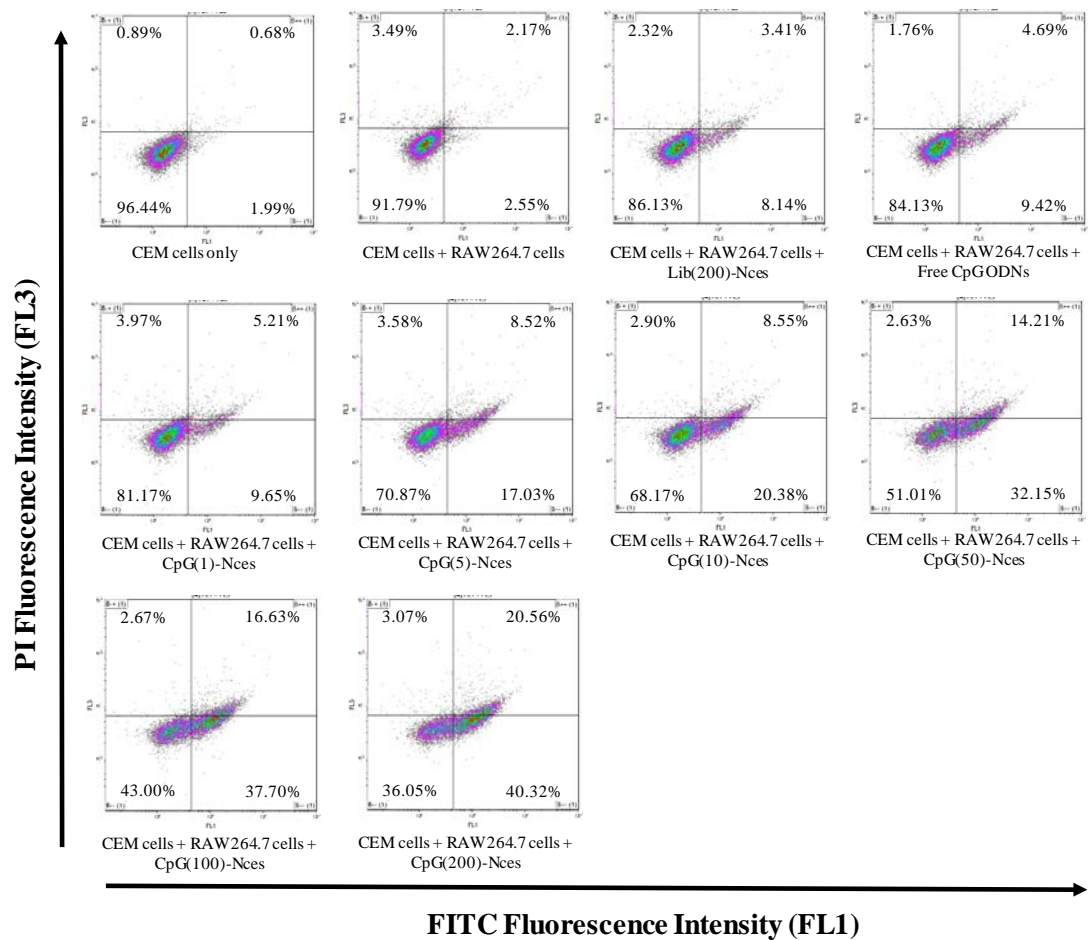


**Fig. S13** The therapeutic effect of CpG-Nces on cancer cells revealed by flow cytometry.

CCRF-CEM (CEM) cells cocultured with RAW264.7 cells and different CpG-Nces at 37 °C for 24 h, respectively, then stained with annexin V-FITC and propidium iodide (PI) followed by flow cytometry analysis.

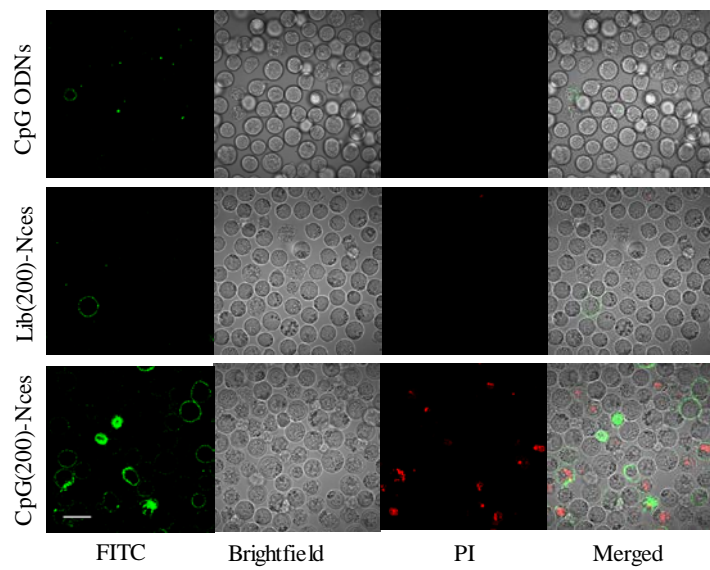


**Fig. S14** The therapeutic effect of CpG(200)-Nces on cancer cells revealed by confocal microscopy.

CEM cells cocultured with RAW264.7 cells and CpG(200)-Nces at 37 °C for 24 h, then stained with annexin V-FITC and propidium iodide (PI), followed by confocal microscopy analysis. Scale bar: 20  $\mu$ m

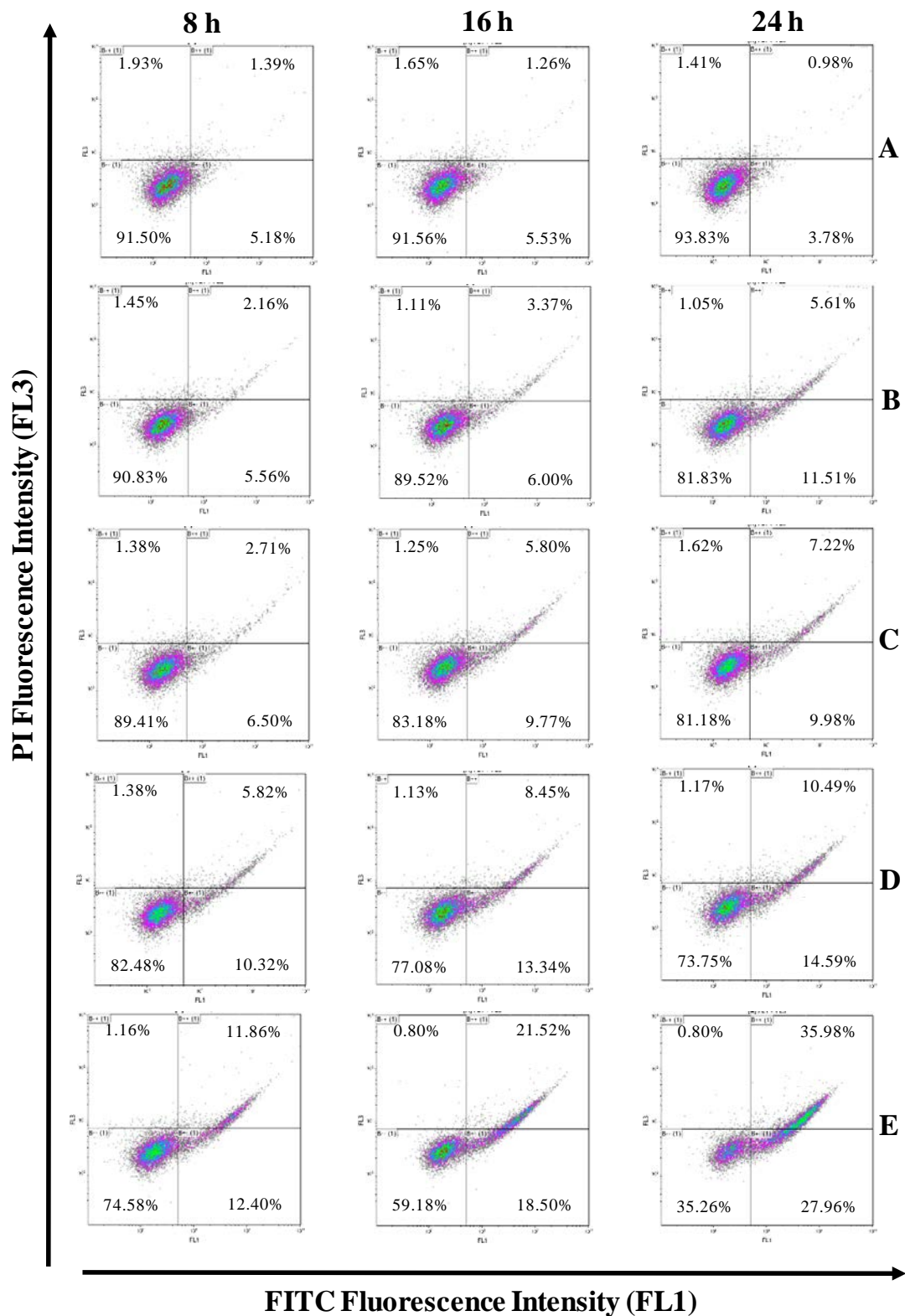


**Fig. S15** Effect of co-culture time on immunotherapy at 37 °C. (A) CEM cells only; (B) CEM cells co-culture with RAW264.7 cells and Lib(200)-Nces; (C) CEM cells co-culture with RAW264.7 cells and free CpG ODNs; (D) CEM cells co-culture with RAW264.7 cells and CpG(1)-Nces; (E) CEM cells co-culture with RAW264.7 cells and CpG(200)-Nces for different times, then stained with annexin V-FITC and propidium iodide (PI), followed by flow cytometry analysis.

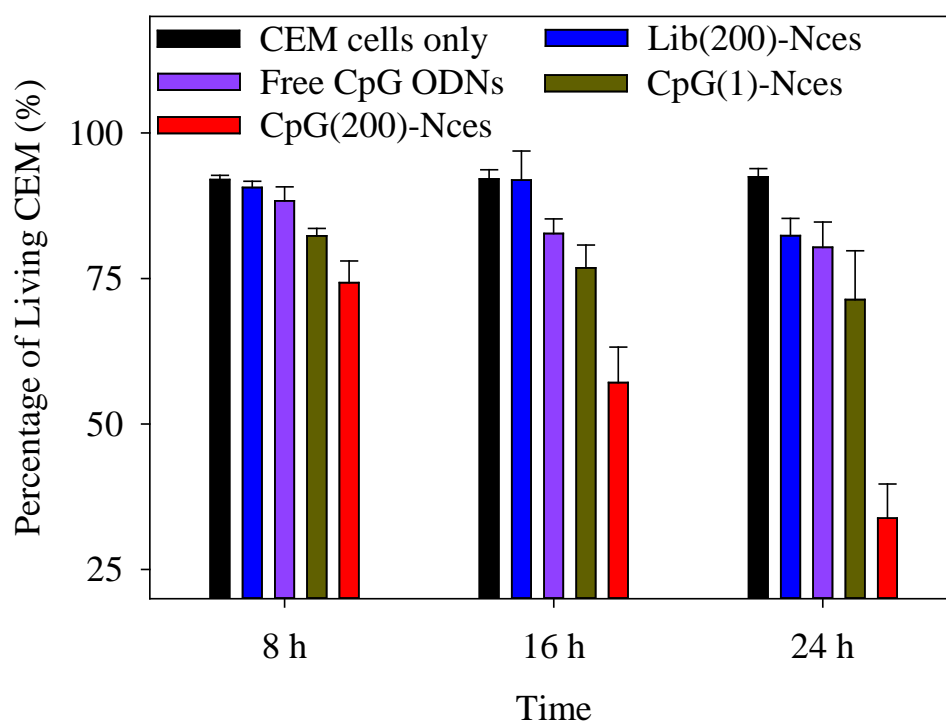


**Fig. S16** Characterization of time-dependent immunotherapeutic effect of CpG(200)-Nces.

CCRF-CEM (CEM) cells co-cultured with RAW264.7 cells and CpG(200)-Nces at 37 °C for different times, then stained with annexin V-FITC and propidium iodide, followed by flow cytometry analysis. The error bars indicated the standard deviations of three experiments.